# We are IntechOpen, the world's leading publisher of Open Access books
# Built by scientists, for scientists

6,900
Open access books available

186,000
International authors and editors

200M
Downloads

154
Countries delivered to

Our authors are among the
TOP 1%
most cited scientists

12.2%
Contributors from top 500 universities

WEB OF SCIENCE™

Selection of our books indexed in the Book Citation Index
in Web of Science™ Core Collection (BKCI)

## Interested in publishing with us?
## Contact book.department@intechopen.com

Numbers displayed above are based on latest data collected.
For more information visit www.intechopen.com

16

# Prediction of Volumetric Shrinkage in Expansive Soils (Role of Remote Sensing)

Fekerte Arega Yitagesu, Freek van der Meer and Harald van der Werff
*International Institute for Geo-information Science and Earth Observation, ITC*
*The Netherlands*

## 1. Introduction

Life time, performance and environmental compatibility of civil engineering infrastructure largely depend on the quality of geotechnical investigations. Apart from being the basis for much of the costing (in terms of time and money both at the construction and maintenance stages) of engineering works, safety of structures lies on information from a geotechnical survey. Existence of expansive soils in construction sites is a great problem that need due consideration in geotechnical investigations.

Expansive soils are weak and unstable when subjected to moisture content fluctuations either due to seasonal climatic variations (cyclic dry and wet periods) or artificial causes. Their presence is one of the crucial factors that can significantly impact engineering costs for it may cause major deterioration and distresses on lightweight and shallowly founded structures. Primary characteristics of expansive soils are their potential to swelling and shrinkage in response to moisture content increase and decrease respectively. These properties are adverse in civil construction works for they pose a huge damage especially on lightweight infrastructures (small buildings, roads and airport runway pavements, pipelines and sewerage systems etc). An increase in volume (swelling) from expansive soils can exceed the downward pressure exerted from lightweight structures and hence cause deformations and development of cracks. Substantial decrease in volume (shrinkage) on the other hand is responsible for uneven settlement. Expansive soils awe their characteristics to their mineralogical assemblage; that is presence of active clay minerals and their amount. Damages due to volume changes of expansive soils in form of swelling and shrinkage that cost billions of dollars are reported in various parts of the world (Al-Rawas, 1999; Erguler and Ulusay, 2003; Gourley et al., 1993; Nelson and Miller, 1992; Ramana, 1993; Shi et al., 2002). Hence expansive soils should be identified and sufficiently characterized at early stages of geotechnical applications in order to guide a detailed design survey so as to avoid or minimize unnecessary expenses and delays in the construction and maintenance of structures.

There are a number of direct and indirect in-situ and laboratory testing procedures available to identify expansive soils and quantify the magnitude of volume change expected. Expansive soils can be identified by surface manifestations in the field, for they show cracks of polygonal pattern in dry seasons (Figure 1) as a result of appreciable volume decrease.

The depth of desiccation cracks are important in indicating the magnitude of volume change since this depth represents the thickness in which moisture deficiency exists upon drying. Various mineralogical identification methods such as X-ray diffraction (XRD), Transmission Electron Micrograph (TEM), Scanning Electron Micrograph (SEM), Differential Thermal Analysis (DTA), dye absorption and chemical analyses are important in research laboratories for exploring the basic properties of clays. But they are costly and hence are not commonly used in soil mechanics laboratories. Direct measurements include determination of swelling and shrinkage potential of expansive soils. Use of consolidation apparatus and triaxial methods are famous for measuring the swelling pressure that is required to counteract the soil swell and swelling potential that can be exerted by the soil expansion. These testing should be done in a sophisticated and controlled conditions with anticipated environmental conditions fulfilled. The techniques give an opportunity of directly observing the effects of soil expansion on different scale or magnitude of loadings that resembles the actual conditions. Suction method can also be used to measure soil swell potential. Volumetric shrinkage determination on the other hand provides with a measure of the magnitude of shrinkage that the soil can undergo upon severe drying. These are the most common and useful swell and heave prediction testing methods (Nelson and Miller, 1992). However, it might take several days and loading steps before the swell pressure is determined even for a single sample which in turn makes the methods expensive and laboursome. Indirect means involve use of index parameters to identify and estimate magnitude of swelling and shrinkage in expansive soils. Atterberg limits (Liquid limit, plastic limit, plasticity indices, shrinkage limit and shrinkage indices) are the most popular and frequently used index tests. Due to the simplicity of these tests and the good correlation that they show with soil swell and shrinkage potentials, Atterberg limits are used in the identification and classification of cohesive soils; as well as directly used in construction specifications and standards (e.g. American Society of Testing Materials (ASTM), British Standard Institution Specification etc) for quality controlling of materials that will be used in fill, embankment and subbase constructions. Cation exchange capacity (CEC), Free swell, Linear shrinkage, Coefficient of linear extensibility (COLE), expansion index (EI), California bearing ratio swell (CBR swell) etc are also some of the index parameters. The more soil testing that is done before hand, the easier it is to reduce risk in the design of infrastructure and produce economically feasible as well as environmentally compatible structures. However it is quite impractical to attempt collecting many samples over short distances and analyze them for it is costly and time consuming.

Fig. 1. Typical expansive soil (black cotton soil of Ethiopia) with polygonal pattern cracks as a manifestation of considerable shrinkage in dry season. These cracks are wide (on the order of tens of centimeters) and also deep (on the order of meters).

Considerable amount of work has been done in the past to support geotechnical investigations of expansive soils with remote sensing techniques (Chabrillat et al., 2002; Goetz et al., 2001; Kariuki et al., 2004; Yitagesu et al., 2009). While Chabrillat et al., (2002) and Goetz et al., (2001) demonstrated potential use of optical remote sensing data for mapping abundances of clay minerals (the three clay species which are smectite, illite and kaolinite that are important with respect to soil swell-shrink potential) responsible for soil swell-shrink characteristics; Kariuki et al., (2004) established one to one relationships between selected engineering parameters of expansive soils and absorption feature parameters. Yitagesu et al., (2009) on the other hand found relationships between engineering parameters (Atterberg limits, cation exchange capacity and free swell) and laboratory acquired spectral reflectance of expansive soils; and indicated wavelength regions to look into in attempting to extrapolate the approach to image datasets for quantitative mapping of soil swell-shrink characteristics.

In this chapter potential use of remote sensing data in modeling volumetric shrinkage and related index properties of expansive soils is illustrated. We presented:

- Possibility of classifying expansive soils with respect to dominant clay mineralogy which is a primary controlling factor in soil swell-shrink characteristics, i.e. to qualitatively characterizing expansive soils.

- Relationships of soil reflectance spectra with geotechnical properties of expansive soils (shrinkage, plasticity and compaction characteristics; grading particularly clay content; and strength or bearing capacity as evaluated by California Bearing Ration (CBR)). Mainly we dealt with prediction of volumetric shrinkage of expansive soils from their respective reflectance spectra.
- A multivariate calibration technique, partial least squares regression (PLSR) model for estimating magnitude of volumetric shrinkage from laboratory acquired (ASD fullrange spectrometer) soil reflectance spectra.

We demonstrated means of identifying soils susceptible to considerable swell and shrink, and propose a simple way of estimating their volumetric shrinkage. Partial least squares regression analysis method is used based on the assumption that volumetric shrinkage and spectral signatures of soils are both a function of clay type and concentration in soil specimens. Empirical relationship between soil volumetric shrinkage and spectral reflectance is presented.

## 2. Methodology

### 2.1 Study area

The study area (Figure 2) is located in the central part of Ethiopia, in the upper valley of the Awash River which drains the northern part of the Rift Valley.

Topography ranges from a relatively plain to hilly, undulating and steep mountainous terrain; with elevation ranging from 1500 to 2500 meters above sea level. Conical-shaped isolated hills of scoria which are products of gas rich mafic lava formed during the late stages of volcanism are common in the study area.

Climate is moderate to wet with mean annual rainfall of 1200 mille meters, and temperature ranging from 25 degree centigrade to 8 degree centigrade. While the temperature is high in January, and from March to May, rainfall is heavy in July and August.

Geology (Abebe et al., 1999) at the start (around TuluDimtu) of the study area is influenced by tertiary to quaternary volcanic formation which includes alkaline basalts, spatter and cinder cones, ignimbrites, rhyolitic flows and domes, and trachyte. Near DebreZeyt the formation is dominated by alluvial and lacustrine deposits which include sand, silt, clay, diatomite and limestone. From DebreZeyt to Mojo town lacustrine deposits, and after modjo town fall and poorly welded pyroclastic deposits dominate with ryolitic and trachytic formations in between.

Soils in the study area are classified into vertisols, luvisols, leptosols, phaeozems and andosols (Figure 1). According to FAO (1998) definitions vertisols are clay rich (smectitic) expanding soils that swell and shrink with fluctuation in moisture content. Luvisols are common soil types in flat or gently sloping land, derived from a variety of unconsolidated material including alluvial, colluvial and eolian deposits. Leptosols are very shallow soils over hard rock or in unconsolidated gravely material, and are most common in mountainous areas. Phaeozems are soils that are predominantly derived from basic material and are rich in organic matter. Andosols are young soils in volcanic regions that are usually associated with pyroclastic parent materials.

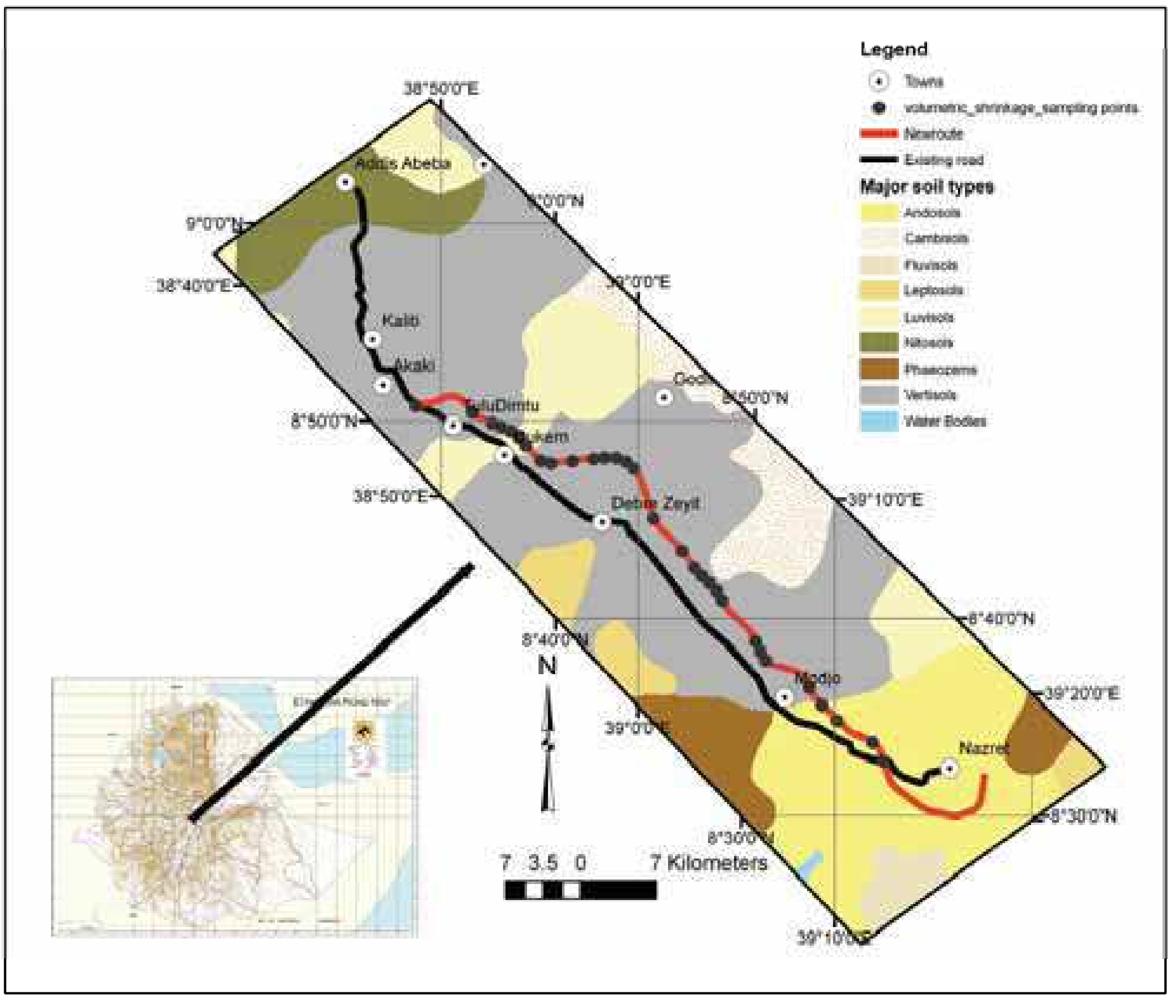


Fig. 2. location map of the study area showing spatial distribution of various soil types, sampling spots are shown following the new highway route to be constructed.

From engineering perspective, soil that are predominately black, highly plastic and expansive clay (vertisol family which commonly termed as black cotton soil) are found during the section from Addis Ababa to Modjo town covering extensive area with varying thicknesses. Thick layers of black cotton soils, which make their susceptibility to volume changes larger, are reported. In these soils prominent desiccation cracks (as shown in Figure 1) are evident in dry periods. While this is the case in the flat to rolling sections, the hilly to mountainous terrains are mainly covered by fresh to partially weathered basalt with minor rhyolitic composition.

Natural vegetation cover is in general poor since most of the area is farmland. An extensive area is farmland with built-up areas following the existing road alignment from Addis Ababa to Nazareth, being the major ones; Kaliti and Akaki (at the outskirts of Addis), Dukem, DebreZeyt, Modjo and Nazareth itself. Deeply incised drainage patterns and gully erosions are common features in the area particularly between Modjo and Nazareth.

### 2.2 Sampling and laboratory testing

Expansive soils mainly distribution of black cotton soils in the study area is so areally extensive thus sufficient detailed characterization is required to aid in formulating proper design and construction techniques. Particularly the amount of volume change (in the form of swelling or shrinkage) should be predicted to eliminate or minimize its detrimental effect on the highway subgrade and associated adverse environmental impacts. Therefore the sampling and laboratory testing strategy was tailored to achieve this aim.

Soil samples were collected following the new express highway from its starting point near TuluDimtu to its end at Nazareth town. The sampling was part of a comprehensive investigation and testing scheme for assessing suitability and quality of subgrade material for the newly proposed road alignment connecting Addis Ababa with Nazareth town. Samples were taken from open pits of one to three meters depth which is commonly the depth at which shallowly founded structures are laid. A total of thirty exploratory pits were excavated.

### 2.3 Determination of geotechnical characteristics

Atterberg limits (liquid limits, plasticity limits and plasticity indices) were determined in accordance with ASTM D4318-05 Standard test method for liquid limit, plastic limit and plasticity indices of soils.

Volumetric shrinkages were determined in accordance with ASTM D4943-02 standard test method for shrinkage factors of soils by the wax method.

Maximum dry density (MDD) and optimum moisture content (OMC) were determined in accordance with ASTM D 689 standard test method for laboratory compaction characteristics of soil using standard effort (12400ft-1bf/ft3 (600KN-m/m3)).

The strength or bearing value of the soil specimen was determined by measuring their California bearing ratio (CBR). Accompanying CBR swell was also measured. The ASTM D1883-05 Standard test method for measuring CBR of laboratory compacted soils is used.

Particle size distributions were determined in accordance with ASTM D6913-04e1 standard test method for particle size distribution (gradation) of soils using sieve analysis (for the fraction passing 2mm, 0.425mm and 0.075 mm ASTM sieve openings); and ASTM D422-63(2007) standard test method for particle size analysis of soils (hydrometer analysis of percent passing 2 μm ASTM sieve opening which is a clay fraction of the soils).

### 2.4 Soil reflectance measurement

ASD fieldspec full range spectrometer (http://www.asdi.com) that covers the 350 nanometer to 2500 nanometer wavelength region of the electromagnetic spectrum was used to collect soil reflectance spectra. The measurement was done in a laboratory, using a contact probe method.

Spectral resolution of the ASD fieldspec FR spectrometer is 3 nanometer for the 350 nanometer - 1000 nanometer region and 10 nanometer for the 1000 nanometer - 2500 nanometer region; whereas its spectral sampling interval is 1 nanometer (ASD, 1995). The spectrometer has three separate detectors, one in the visible near infrared region (VNIR) and the two are in the short wave infrared (SWIR) region. Since major absorption features associated with clay minerals are found in the SWIR wavelength region of the electromagnetic spectrum, clay minerals are among the mineral groups that are suitable for

ASD analysis. Additional spectral information can also be obtained from the VNIR wavelength regions.

### 2.5 X-Ray Diffraction (XRD) analysis

Mineralogical composition of soil samples were examined using X-ray diffractometer (XRD). The instrument used is Siemens D5000 diffractometer. Bulk (to determine the overall constituents) as well as clay fractions (to quantify the major, minor and trace composition of clay species) of the soil samples were analyzed.

### 2.6 A multivariate analysis Partial least squares regression (PLSR)

Partial least squares regression (PLSR) is regression by means of projections to latent variables (Martens and Naes, 1989; Wold et al., 2001). The method was first proposed in the 1970's, and is currently very popular in various disciplines, among which is spectroscopy. In visible near infrared spectroscopy, PLSR has become a widely spread technology for qualitative as well as quantitative analysis. This includes routine quality control activities; in chemical, pharmaceutical and agro-industries, for it is found to be a fast, cheap, simple and non-destructive technique with little or no sample preparation requirements.

PLSR is particularly important when dealing with a large number of variables that express common information to avoid multicollinearity problems (Martens and Naes, 1989). It reduces the impact of irrelevant X variation in the calibration modeling by balancing the information in the X and Y spaces. This is especially the case when one acquires a large data set using modern instrumentation like spectrometers, where, apart from having numerous X-variables, there is also a tendency of these variables for being correlated, sometimes being noisy and incomplete (Wold et al., 2001). On the other hand, the need to use PLSR analysis method can arise from difficulty to obtain measurements only of the specific parameters that one is interested in. Martens and Naes (1989) discussed problem of selectivity while trying to take measurements of specific properties from inhomogeneous materials and presented a multivariate calibration method, PLSR as a solution. PLSR combine principal component analysis (PCA) and multiple linear regressions (MLR). In this technique X-variables are first decomposed into set of orthogonal factors named latent variables. During the decomposition the common structures between predictors and response is captured. Unlike PCA which decomposes the X variables to eliminate multi-collinearity problems and extract components that explain X, PLS finds components from X that are also relevant to Y. Since PLSR considers the variation in Y when calibrating the model, the covariance structure between the predictor and response variables is reflected (Martens and Naes, 1989; Wold et al., 2001). This is achieved by projecting the X and Y-spaces into new coordinates T and U-scores respectively that summarize the common structure in X and Y. Thus resulting latent variables have the best predictive power in explaining the response. Then as in multiple linear regression it builds a linear model $Y=XB+E$, where Y is an n cases by m variables response matrix, X is an n cases by p variable predictor matrix, B is a q by m regression coefficient matrix, and E is a noise term for the model which has the same dimensions as Y (Wold et al., 2001).

Prior to considering the calibrated models for practical applications, i.e. the prediction and subsequent understanding of new data set or samples, models should be validated (Wold et al., 2001). This is a crucial step in PLSR modeling, for it gives an indication on how well the

models will perform in the future and the degree of certainty that one might expect while using the models to solve practical problems. Different types of validation methods were discussed and presented in various literature (Martens and Naes, 1989; Wold et al., 2001). Of which, cross validation method has found its application in cases where the data set that one is working on is small and hence a separate or independent and representative validation data set is unavailable (Martens and Naes, 1989). Kooistra (2005) used a full cross validation method, which is based on a leave one out principle where one sample will be left out at a time and the model is calibrated on the remaining samples (CAMO, 2005). This will be repeated N times until every sample is left out once and the model is computed on the remaining samples and the left out sample is predicted.
To avoid erroneous calibration and deterioration of models prediction ability, it is important to detect outliers and remove or replace them by accurate values (Hocking, 2003; Martens and Naes, 1989). Outliers are abnormal observations that show significant deviation from the rest of the dataset in the population. They might arise both due to error in the experiment or instrument, or represent different information other than the material of interest and hence irrelevant. Presence of outliers in the data set is known to influence both the calibration and validation of PLSR models. Different methods are developed to detect sample outliers in PLSR modeling. Martens and Naes (1989) presented outlier detection criteria based on the analysis of residuals and leverages. In PLSR modeling, residuals are of diagnostic interest. It is possible to examine the residual variances (the variation that is left unexplained) in the X as well as the Y-spaces. Wold et al. (2001) demonstrated that large Y-residuals indicate that the model is poor. Normal probability plots of the residuals of a single Y-variable are also useful for identifying outliers in the relationship between T and Y. The X-residuals (part of X that is not used in modeling Y) are also useful for identifying outliers in the X-space, i.e., observations that do not fit the model. In addition, uncertainty tests e.g. Martens uncertainty limit tests (CAMO, 2005; Martens and Naes, 1989) can be used for testing which variables are causing perturbations in the model.

## 3. Results and Discussions

### 3.1 Spectral analysis

In the spectral interpretations, spectral libraries of different sources (e.g. TSG (the spectral geologist), ENVI and PIMA view built-in mineral libraries, USGS and JPL mineral libraries) that are developed upon experimental investigations on minerals and verified with variety of conventional testing methods (e.g. X-ray diffraction (XRD), Transmission Electron Micrograph (TEM), Scanning Electron Micrograph (SEM) etc) are used.
Differences in spectral characteristics among spectra of different soil samples were used for differentiating various clay mineral types that are present in the soil samples. Position of absorption features, their shapes, types and number, depth intensity and asymmetry; shape of spectral curves, differences in slopes of spectral curves and variations in reflectance intensity of spectra were some of the important qualitative parameters that helped in identifying spectrally dominant clay mineral from the soil reflectance spectra (Figure 3). Some spectra show a sharp rise in slopes and variable reflectance intensity throughout the whole wavelength region of the electromagnetic spectrum. Others show lower reflectance intensity throughout the whole wavelength range and were on overall dark. The later also exhibited monotonously rising convex slopes in the VNIR (visible near infrared) wavelength

region and less variable reflectance intensity in the SWIR. Some show moderate rise in slopes and also moderate increase in reflectance intensity from the VNIR to the SWIR wavelength regions.
In the visible near infrared portion of the spectra changes in slopes were the prominent features that were recognized coupled with changes in reflectance intensities. The absorption features that are apparent on the VNIR region are relatively few, broad, wider and less intense. Whereas, in the SWIR region the main absorption features of clay minerals were observed with variable intensity being the prominent ones at ~ 1400 nanometer, ~ 1900 nanometer and ~ 2200 nanometer (Clark, 1999; Van der Meer, 1999).

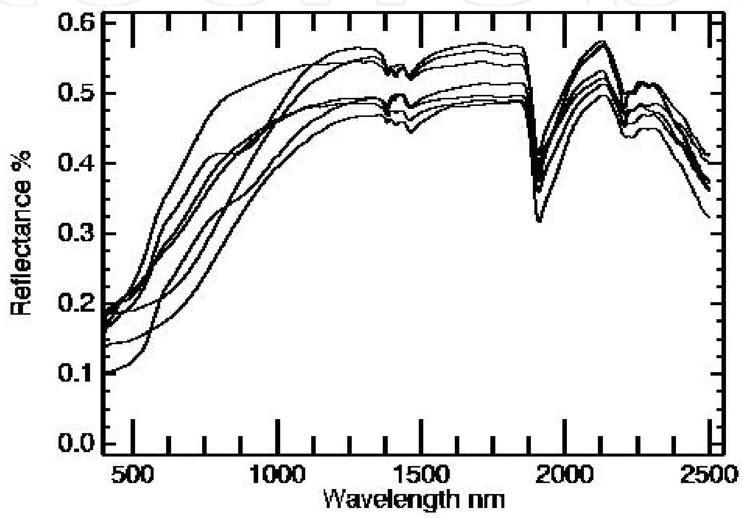


Fig. 3. Spectral reflectance curves of some soil samples (no offset). Note spectral characteristic differences, reflectance and slope variability in the VNIR wavelength region (350 nanometer – 1000 nanometer) and absorption features in the SWIR (1000 nanometer – 2500 nanometer).

### 3.2 Geotechnical Characteristics

As presented in the plasticity chart (Figure 4) and particle size distribution of soil samples (Figure 6), the soil samples exhibit high plasticity and are finer grained with high percentages of clay fraction. Generally the more plastic and finer grained soils are the greater swell-shrink potential that they are susceptible to, though swell-shrink potential is dictated by mineralogy and other factors as well. Majority of the soil samples are plotted above the A-line spanning from CI to CE zones. The soils that fall in the CI zone are of intermediate plasticity behavior, while those falling in the CH, CV and CE are of high, very high and extremely high plasticity nature. The higher the plasticity the larger will be the susceptibility of the soil to significant volume change characteristics. Accordingly swell-shrink potential of soil samples in the CH, CV, and CE zones are of high, very high and extremely high. Few samples fall below the A-line in the MV zone; these soils have high inherent expansion potential. The 'A' line is an empirical boundary separating inorganic clays from silty and organic soils. Soils of the same geological origin usually plot on the plasticity chart as straight lines parallel to the 'A' line. "Fat" or plastic clays plot above the line. Organic soils, silts and clays containing a large portion of "rock flour" (finely ground non-clay minerals) plot below it.

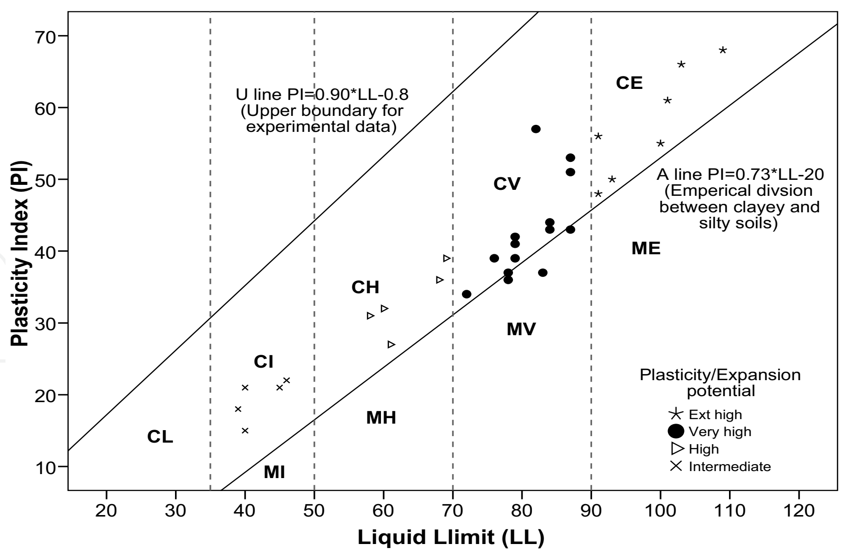


Fig. 4. Plasticity chart showing classes of expansion potential of soil samples.

The scattering of soil specimen in the plasticity chart show a wide range of variability in their swell-shrink characteristics (low to extreme cases). This is important in ensuring representativeness of samples for the intended PLSR modeling since it affects model prediction ability (Martens and Naes, 1989). Calibration in narrow range can bring about a risk of inability to extrapolate model into observations spanning a wider range. That is for instance bad prediction ability in case of failing to cover a total range of variability in a new dataset.

Proctor test results of some soil samples depicting the maximum dry density (MDD) and optimum moisture content (OMC) are shown in Figure 5. As presented in the graph the soil samples are also labeled with mineralogical groups obtained upon interpretation of spectral reflectance curves of respective soil samples.

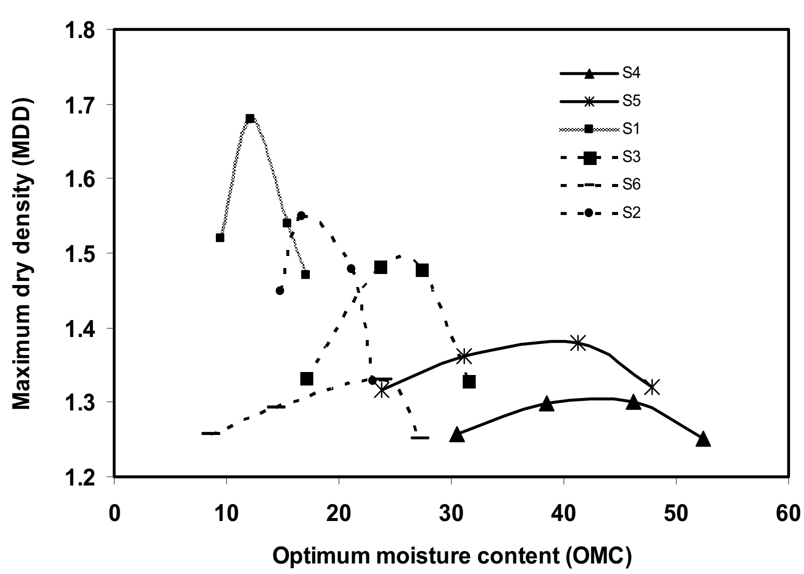


Fig. 5. Compaction curves of selected soil samples from proctor test labeled with mineralogical classes of soil from spectral interpretation.

Smectite clay species dominated soils (S4 and S5) exhibited low dry densities (MDD) with large moisture intake as indicated by their optimum moisture contents (Figure 5). As the grading curves (Figure 6) depicted S4 is finer than S5 with higher clay content. Accordingly S4 shows higher magnitudes of volumetric shrinkage and plasticity character (LL, PI) than its similar species S5 (Table 1).
Halloysite dominated soils (S2, S3 and S6) are characterized by dry densities and moisture intakes that seem to vary with their clay contents. While S6 has highest clay content of the three soils followed by S3 and S2 (Figure 6), the magnitude of volumetric shrinkage and plasticity that it exhibited is also high followed by S3 and S2 (Table 1). Dry density of S2 is the highest followed by S3 and S6 respectively (Figure 5) in the halloysite clay dominated sols.
The quartz dominated soil (S1) attained the highest dry density with lowest moisture intake as compared with soils dominated by halloysite and smectite clay varieties (Figure 5). This soil is also coarser than the other soils (Figure 6) and is non-expansive (Table 1).

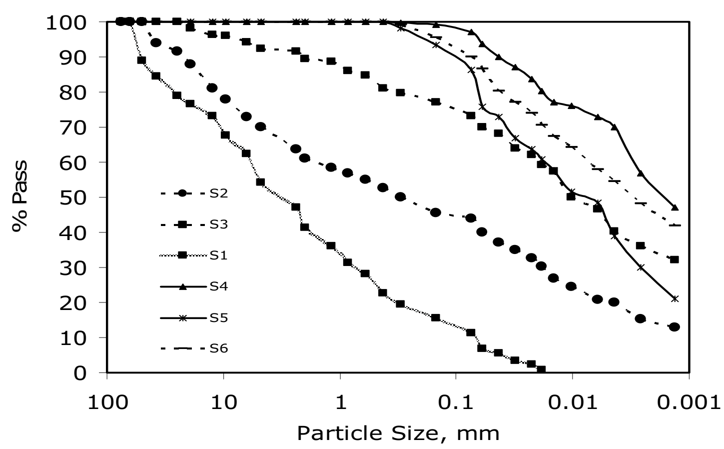


Fig. 6. Particle size distributions of selected soil samples labeled with mineralogical classes of the soil specimen obtained from spectral interpretation.

Even though the clay content of halloysite dominated soil sample S6 is higher than the clay content of smectite dominated soil sample S5, the later is characterized by higher magnitudes of volumetric shrinkage and plasticity, and exhibited low dry density (MDD) coupled with high moisture intake (OMC). This observation can be attributed to the fact that clay mineralogy dominantly controls swell-shrink characteristics of expansive soils. On the other hand within similar clay mineralogy, amount of clay fraction seems to govern the magnitude of volumetric shrinkage, plasticity (LL and PI) and compaction characteristics (MDD and OMC).

| Sample ID | Spectrally dominating mineral | Volumetric shrinkage | Liquid limit | Plasticity index |
|---|---|---|---|---|
| S4 | smectite | 137 | 103 | 58 |
| S5 | smectite | 118 | 84 | 43 |
| S6 | halloysite | 99 | 72 | 34 |
| S3 | halloysite | 48 | 48 | 22 |
| S2 | halloysite | 32.8 | 46 | 22 |
| S1 | quartz | - | Np | Np |

Table 1. summary of geotechnical properties of selected soil samples. NP: non plastic material

Variations in CBR and CBR swell of the six soil samples from different mineralogical groups are presented in Figure 7. The CBR value is an indicator of soils strength or bearing capacity, which is directly used in the design of subgrade, subbase and base material for pavement. Highest CBR and lowest CBR swell values are attained by the quartz dominated soil sample, S1. For the smectite dominated soils (S4 and S5) lowest CBR and highest CBR swell values are recorded. CBR of S4 and S5 are below standard (e.g. to lay an embankment directly over or to be used as subgrade material in road construction) and their CBR swell is much higher than allowable CBR swell values. Halloysite dominated soils (S2, S3 and S6) exhibited CBR and CBR swell values which seems to vary according to their clay fractions. Among the halloysitic soils S6 show low CBR which is below standard and higher CBR swell which is higher than the allowable CBR swell value. S3 on the other hand exhibited marginal CBR value with high though within the allowable range in different standard specifications.

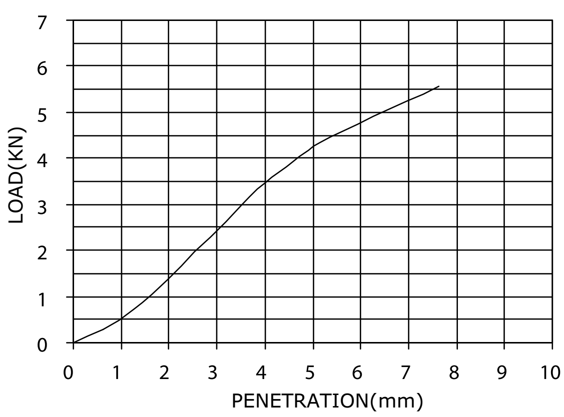


| ID | Penetration (mm) | load (KN) | Standard load (KN) | CBR (%) | CBR Swell (%) |
|---|---|---|---|---|---|
| S1 | 2.5 | 1.98 | 13.24 | 14.95 | 0.31 |
| | 5 | 4.36 | 20 | 21.80 | |

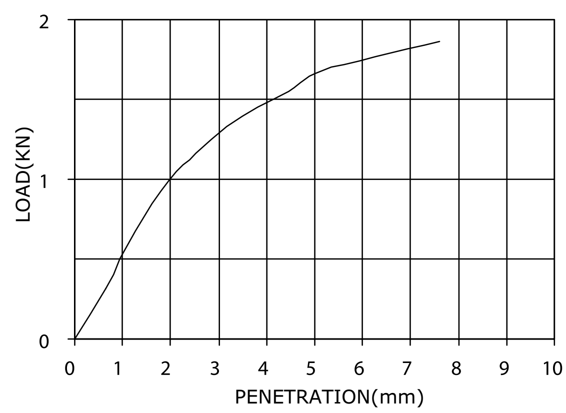


| ID | Penetration (mm) | load (KN) | Standard load (KN) | CBR (%) | CBR Swell (%) |
|---|---|---|---|---|---|
| S2 | 2.5 | 1.16 | 13.24 | 8.76 | 0.94 |
| | 5 | 1.67 | 20 | 8.35 | |

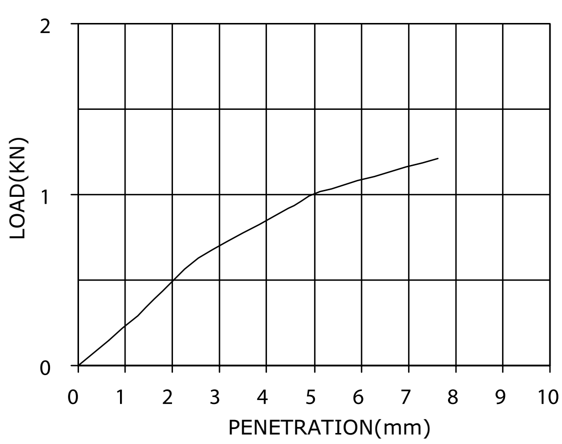


| ID | Penetration (mm) | load (KN) | Standard load (KN) | CBR (%) | CBR Swell (%) |
|---|---|---|---|---|---|
| S3 | 2.5 | 0.63 | 13.24 | 4.76 | 1.89 |
| | 5 | 1.02 | 20 | 5.10 | |

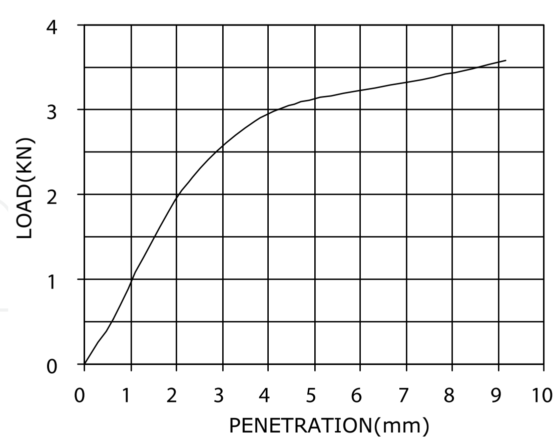


| ID | Penetration (mm) | Load (KN) | Standard load (KN) | CBR (%) | CBR Swell (%) |
|---|---|---|---|---|---|
| S4 | 2.5 | 0.14 | 13.24 | 1.06 | 14 |
| | 5 | 0.19 | 20 | 0.95 | |

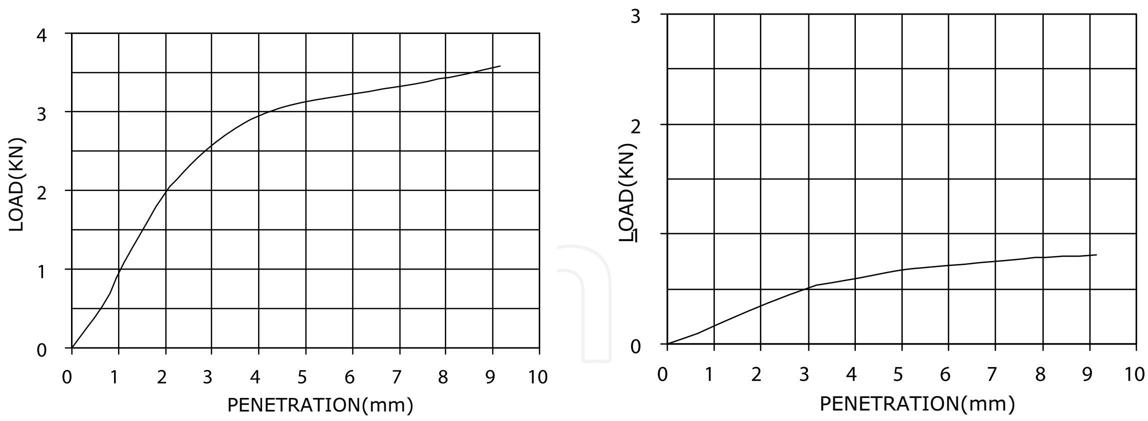


| ID | Penetration (mm) | Load ( KN) | Standard load (KN) | CBR (%) | CBR Swell (%) |
|---|---|---|---|---|---|
| S5 | 2.5 | 0.44 | 13.24 | 3.32 | 10 |
| | 5 | 0.54 | 20 | 2.70 | |

| ID | Penetration (mm) | load (KN) | Standard load (KN) | CBR (%) | CBR Swell (%) |
|---|---|---|---|---|---|
| S6 | 2.5 | 0.44 | 13.24 | 3.32 | 4.29 |
| | 5 | 0.68 | 20 | 3.40 | |

Fig. 7. CBR and CBR swell results, graphs with accompanying tables.

XRD test results show that the soil samples contain clay minerals (Figure 8) such as smectite (mainly montmorillonite and nontronite), illite and kaolinite (halloysite and kaolinite) which significantly influence engineering behavior of expansive soil due to their high activity; and original minerals such as quartz, feldspar and mica are which are common constituents of expansive soils but do not contribute to the expansiveness of soils due to their low activity. Qualitative XRD analysis results are summarized in Table 2 and chemical analysis results are resented in Table 3.

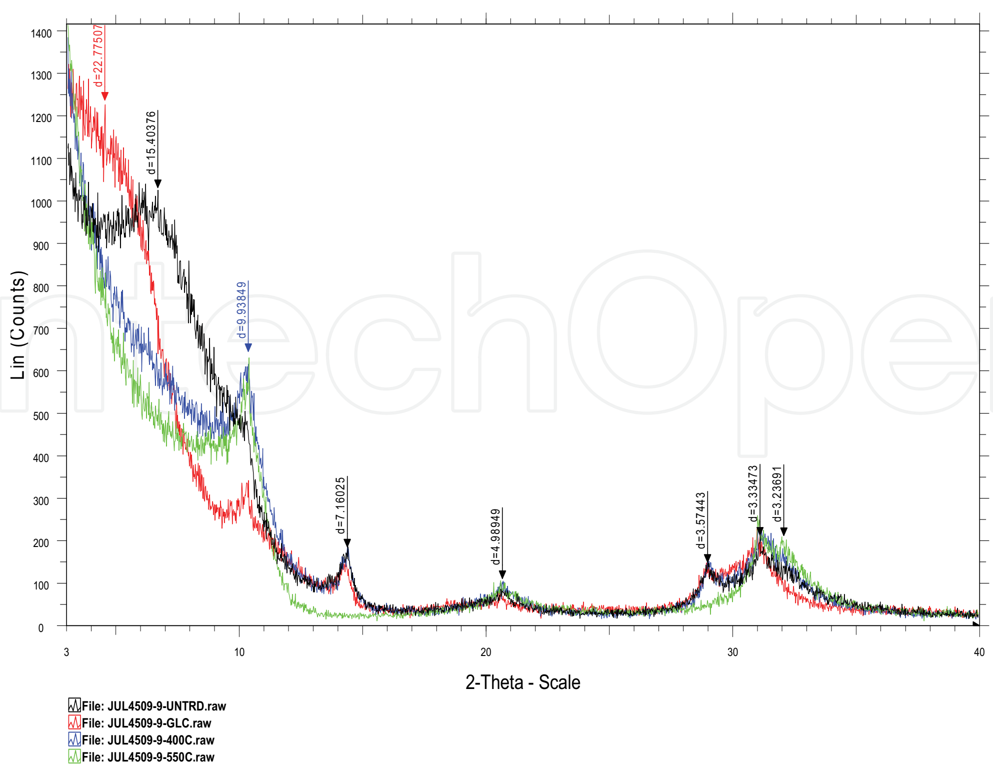

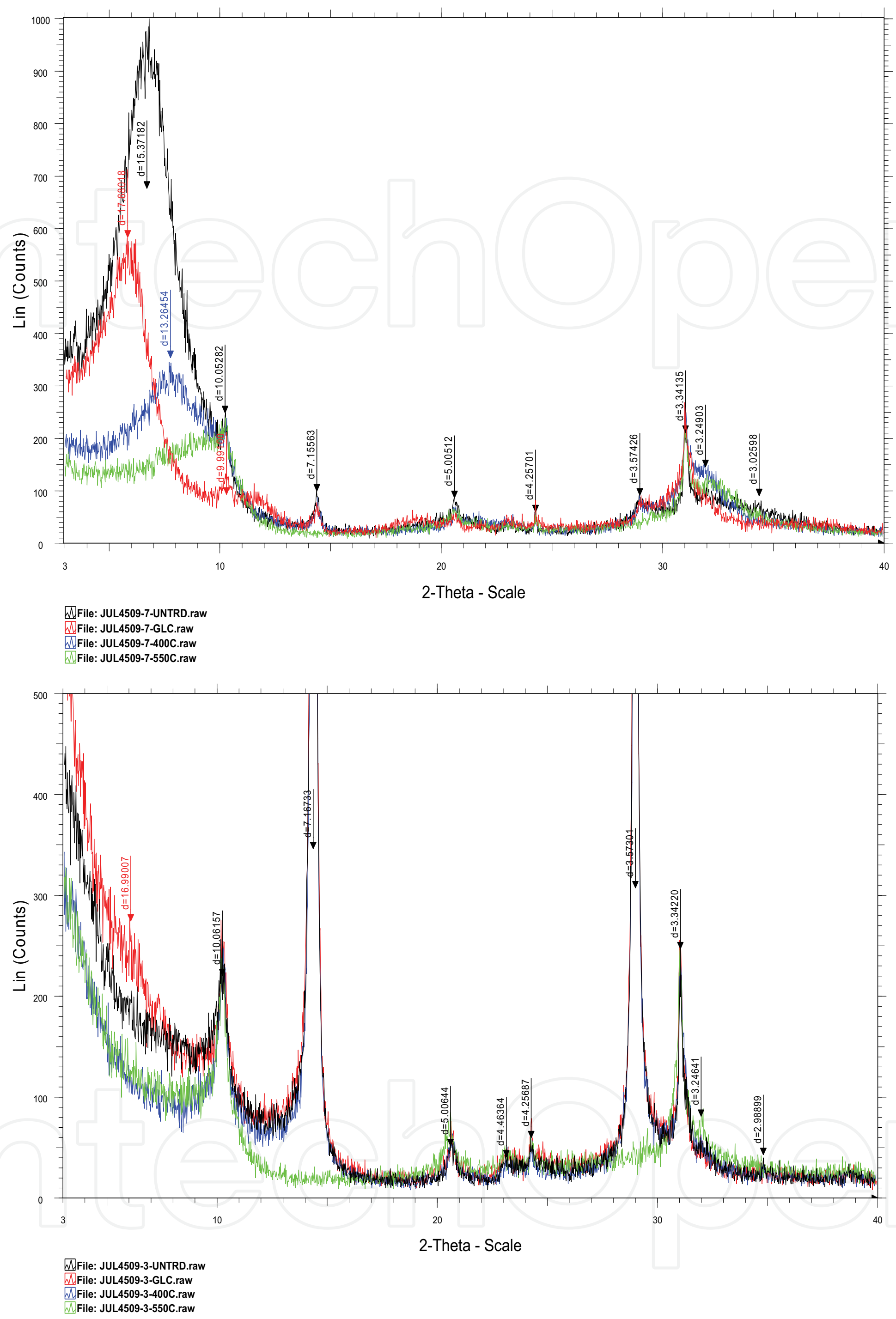


Fig. 8. XRD patterns of clay fractions (< 2μ) of some soil samples (Table 2 and 3 present the mineralogical assemblage and chemical results of these three patterns in descending order).

| ID | | XRD mineralogy assignment | | | | Spectrally dominant mineralogy |
|---|---|---|---|---|---|---|
| | | **Major** | **Moderate** | **Minor** | **Trace** | |
| 1 | **Bulk** | Montmorillonite | quartz, calcite, Nontronite | kaolinite, plagioclase, potassium feldspar, Illite | *brookite, *rutile, *goethite | Smectite |
| | **Clay Fraction** | Montmorillonite | - | illite, kaolinite, (quartz), (calcite), (potassium feldspar) | - | |
| 2 | **Bulk** | Montmorillonite | quartz, Nontronite | kaolinite, plagioclase, potassium feldspar, Illite | *brookite, *rutile, *goethite | Smectite |
| | **Clay Fraction** | I/M mixture | Nontronite | illite, kaolinite, (quartz), (calcite), (potassium feldspar) | - | |
| 3 | **Bulk** | - | quartz, kaolinite, halloysite | potassium felspar, illite, plagioclase, montmorillonite, nontronite, I/M mixed | *brookite, *pyrite, *goethite | Halloysite |
| | **Clay Fraction** | Halloysite | - | (quartz), illite, I/M mixed | *montmorillonite, *(potassium feldspar) | |

Table 2. Summary of Qualitative XRD results showing abundance of major (>30%), moderate (10 -30 %), minor (2 – 10 %) and trace (< 2 %) mineral constituent of soil samples.

| ID | Sio2 % | Al2O3 % | Fe2O3 % | MgO % | CaO % | Na2O % | K2O % | TiO2 % | P2O5 % | MnO % | Cr2O3 % | V2O5 % | LOI % | Sum % |
|---|---|---|---|---|---|---|---|---|---|---|---|---|---|---|
| 1 | 46 | 13.8 | 7.14 | 2.29 | 5.66 | 0.79 | 1.46 | 1.14 | 0.08 | 0.18 | 0.02 | 0.02 | 21.4 | 99.98 |
| 2 | 50.8 | 16.9 | 8.46 | 1.5 | 1.33 | 2.16 | 2.53 | 1.03 | 0.04 | 0.24 | 0.01 | 0.02 | 14.5 | 99.52 |
| 3 | 52.9 | 19 | 7.95 | 1.63 | 0.3 | 0.77 | 1.86 | 1.22 | 0.15 | 0.17 | 0.01 | 0.02 | 13.2 | 99.18 |

Table 3. Chemical analysis results.

The information obtained on the clay mineralogical assemblage of the soil samples from X-ray diffraction analysis is in conformity with spectrally dominant mineralogical group assignments from interpreting reflectance spectra of respective soil samples.

Major clay mineral that is responsible for swelling and shrinkage of soils in the study area is smectite (montmorillonite and nontronite) as identified from soil spectral reflectance and confirmed by the X-ray diffraction analysis; and mixed layer combination of montmorillonite and illite. The hydrous variety of kaolinite group (halloysite) shows variable, that is low to appreciable swell-shrink character. Halloysite show low bulk density than kaolinite coupled with high porosity; its hydraulic conductivity is also reported to be higher (West et al., 2004). Geotechnical character of halloysite dominated soils seems to vary according to their particle size distribution (clay to coarser fraction proportions).

Montmorillonite, $(Ca, Na)_{0.67}Al_4(Si, Al)_8O_{20}(OH)_4 \cdot nH_2O$, is a product of weathering of iron and magnesium rich parent materials and is one of the most common smectite minerals (AusSpec International, 2005; Fitzpatrick, 1980) found in soils. It also form from the weathering of volcanic ash or primary silicate minerals such as feldspars, pyroxenes, or amphiboles under conditions of insufficient leaching of soil profile due to low permeability and excessive evaporation (Snethen, 1975). As indicated in the brief summary of the Geology of the study which is covered by rocks of volcanic origin where volcanic debris and mafic rocks like basalt are common and abundant, occurrence of montmorillonite can be favored by the environment. Nontronite, (Ca, Na) 0.66 Fe3+4(Si, Al) 8O 20(OH) 4 ·nH2O, is also a common smectite mineral found in soils and weathered bedrock. Its formation is favored by alkaline to neutral pH environments, as well as by the availability of iron and calcium minerals (AusSpec International, 2005; Fitzpatrick, 1980). Thus its formation is also favored by the geology of the study area. Additional prevailing environmental conditions such as alkaline conditions coupled with high evaporation exceeding precipitation and poor leaching which facilitate retention of magnesium and calcium in the soils contribute to the development of smectite clays in the area.

Kaolinite, Al2Si2O5 (OH)4 is another commonly occurring clay mineral in soils. It can be derived from almost all silicate minerals (AusSpec International, 2005), hence its formation in the study area can be favored by the environmental conditions. Halloysite, Al2Si2O5(OH)4·4H2O, occurs in soils and the uppermost weathered part of bedrock (AusSpec International, 2005) and is a common constituent of many volcanic soils (Takahashi et al., 2001). It is a kaolinite group clay mineral formed as a result of weathering of aluminum rich minerals that are also abundant in the study area and its surroundings.

Illites on the other hand are commonly seen in soils, and form by weathering of silicates primarily feldspars. Generally their formation is favored by alkaline environment and high concentrations of Aluminum and potassium (Fitzpatrick, 1980); which are conditions fulfilled in the study area. It is common that illites appear with smectitic interlayer clays (AusSpec International, 2005).

Some spectra show presence of iron oxides in the soil samples. Different kinds of iron oxides, for example, goethite (αFeO+3(OH)) is present (Figure 3 and Tables 2 and 3) in the soil samples as a result of weathering product of iron-bearing minerals. Since volcanic rocks that are rich in iron minerals are abundant in the study area; which is coupled with the action of chemical weathering in the humid atmosphere of the local tropical climatic conditions; presence of goethite in the soil samples can be favored by the environmental conditions. Spectra of some soil samples showing diagnostic features of iron oxides similar to the spectral characteristics of goethite (Crowley et al., 2003) can be seen in Figure 3.

Figure 9 presents relationships between magnitudes of soil volumetric shrinkage; soil mineralogical group resulted from spectral reflectance interpretation and plasticity classes according to the plasticity chart. Mean volumetric shrinkage of smectite dominated soil samples is higher than that of the halloysite dominated ones. The two mineralogical classes that the soil samples are grouped into show clear separation. The halloysite dominated soils fall into the intermediate and high plasticity classes which denoted intermediate and high swell-shrink susceptibility. Smectite dominated soils on the other hand fall within the extremely high and very high plasticity classes with few samples falling in the high plasticity class signifying extremely high, very high and high swell-shrink potential respectively. Even though few smectitic soils are noted to belong in the high plasticity class, mean volumetric shrinkage of these soils is higher (~ 120) than the mean volumetric shrinkage of halloysitic soil samples which is about 80. The whiskers of boxes denoting high plasticity class of halloysite rich soils and very high class of smectite rich soils suggesting some overlap on the magnitude of volumetric shrinkage of the two classes though fall within different mineralogical categories. This might be related with high clay content of halloysite rich soil samples and low clay fraction of those of smectite rich soils. Takashi

(2001) reported halloysite rich volcanic soils with appreciable clay fraction exhibiting high cation exchange capacity indicating high swell-shrink potential.

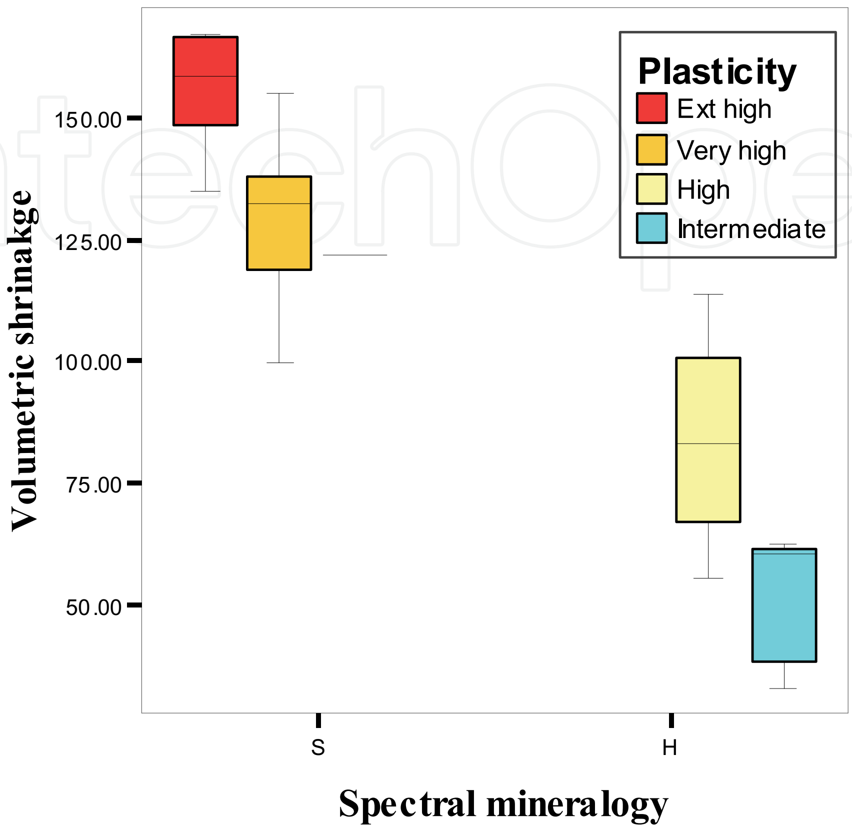


Fig. 9. Relationships between volumetric shrinkage, mineralogy and plasticity of the soil samples. Note an increase in magnitude of volumetric shrinkage as mineralogy changes to highly expanding clay species (smectite) dominated soils, coupled with increase in mean volumetric shrinkage as plasticity changes from intermediate to high, very high and extremely high classes.

Smectite and halloysite rich soils fall into two distinct clusters while plotting the values of liquid limit (LL) in the X-axis against the magnitude of volumetric shrinkage in the Y-axis (Figure 9). K-means clustering (which is a procedure that attempt to identify and cluster homogeneous groups based on distance from specified or computed cluster centers) also gave these two clusters with LL of 65 and volumetric shrinkage of 100 as boundaries separating the two clusters. Same kind of clustering is noted in the plots showing the relationship between Plasticity indices (PI) versus volumetric shrinkage. Sample labeling 1 and 2 in each graph are cluster designations obtained from the K-means clustering analysis.

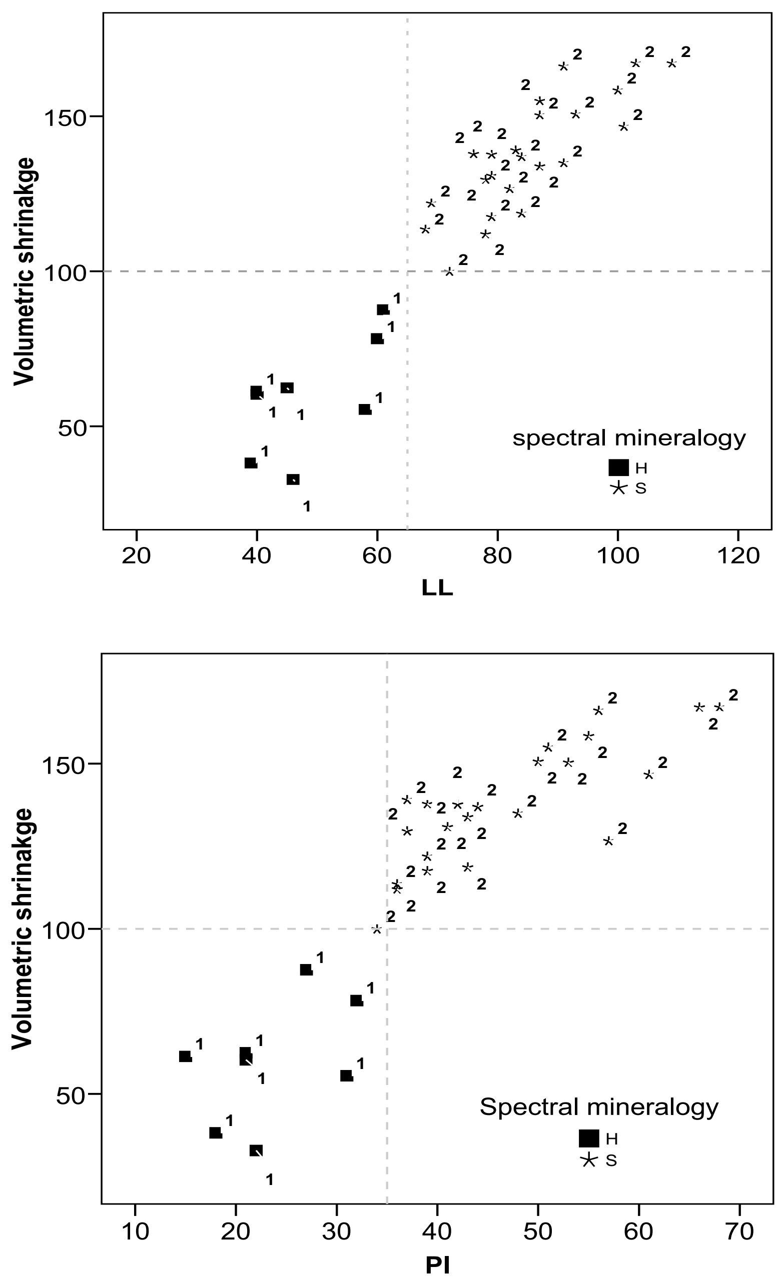


Fig. 10. Scatter plots showing the relationships between volumetric shrinkage versus liquid limit, and volumetric shrinkage versus plasticity index with samples labeled with mineralogical classes. Sample labeling 1 and 2 are cluster designation obtained from K-means clustering analysis.

### 2.5 Partial Least Squares Regression (PLSR) models

PLS1 analysis (predicting a single parameter at a time) method implemented in The Unscrambler software (CAMO, 2005) was used for the multivariate calibration and validation. Outlier detection was performed, since presence of outliers in the input dataset can deteriorate models prediction ability and also their reliability. Outliers were mainly identified manually instead of using the automatic outlier detection method. The automatic detection tends to include many of the extreme values (either from the lower or higher extremes) in the outliers list. In general outlier detection was done based on using a combination of different tests rather any single method. We used Martens uncertainty limit tests to test the stability of all variables in the model. The stability of each predictor with respect to the samples was examined by using stability plots.

A sufficient number of PLS factors were used, that is three PLS factors with optimal predictive ability. Including too many PLS factors was observed to often lead to over fitting problems (Kooistra, 2004) for it incorporates irrelevant information or noise. The number of PLS factors used in the models were based on different tests intended for testing the significance of PLS factors in the prediction. Among the tests are simultaneous examinations of the residual variances and the root mean square errors (RMSE) of each factor coupled with significance tests through cross validation. Cross validation is a practical and reliable way of testing the predictive significance of PLS factors analysis (Martens and Naes, 1989) that has become a standard in PLS (Wold et al., 2001). Martens and Naes (1989) demonstrated the application of cross validation methods for determining number of PLS factors that should be included in a model for proper explanation of the phenomena of interest that one would like to model.

In deciding which variables, among the predictors, should be retained in the model, Martens uncertainty limit test was used. This test is significance test in PLS analysis which is useful in testing whether the regression coefficients used in a model are significantly contributing to the model. Regression coefficients that are significant were then identified and those that have got an uncertainty limits passing the origin were left out. Another uncertainty test that was applied on the score and loading plots was stability calculation which can be visualized in The Unscrambler as stability plots. It shows the influence of each variable and hence its significance (CAMO, 2005) in the model. Samples far from the center have more influence on the model than those that are near, and the uncertainty is larger on those with larger spread implying that these variables are not significant (CAMO, 2005).

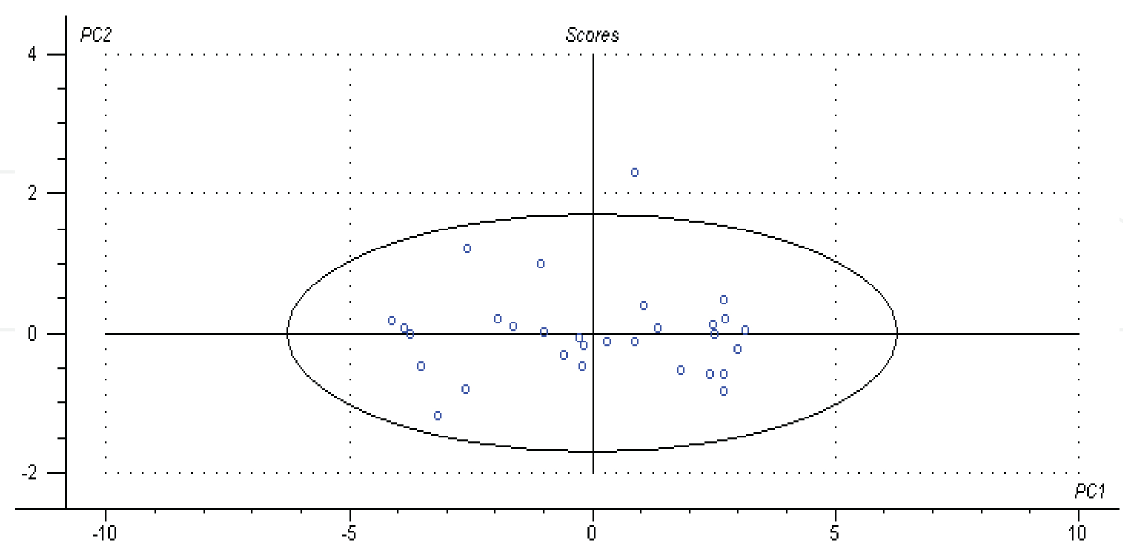


Fig. 11. Result of PLSR modeling for volumetric shrinkage showing: Scores principal components 1 versus 2 with samples in the 95% confidence ellipse showing that there is no particular grouping of samples, but rather a random pattern (one population) suggesting a single model can fit the data.

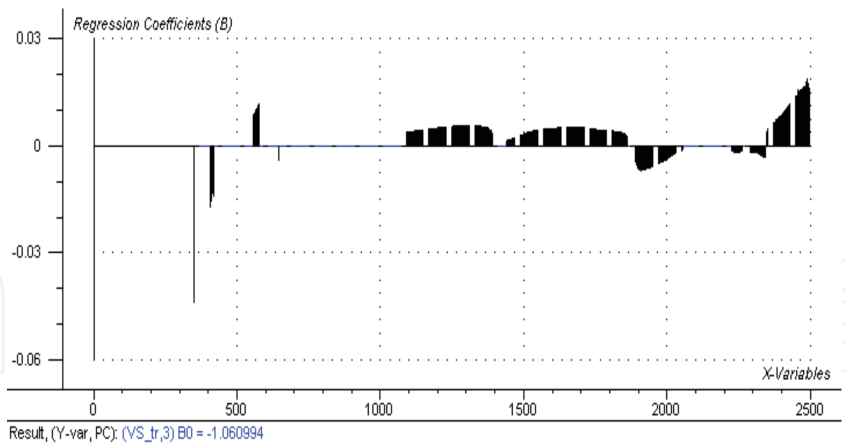


Fig. 12. Result of PLSR modeling for volumetric shrinkage showing: Regression coefficients or statistically significant wavelength regions in predicting volumetric shrinkage from the laboratory soil reflectance spectra.

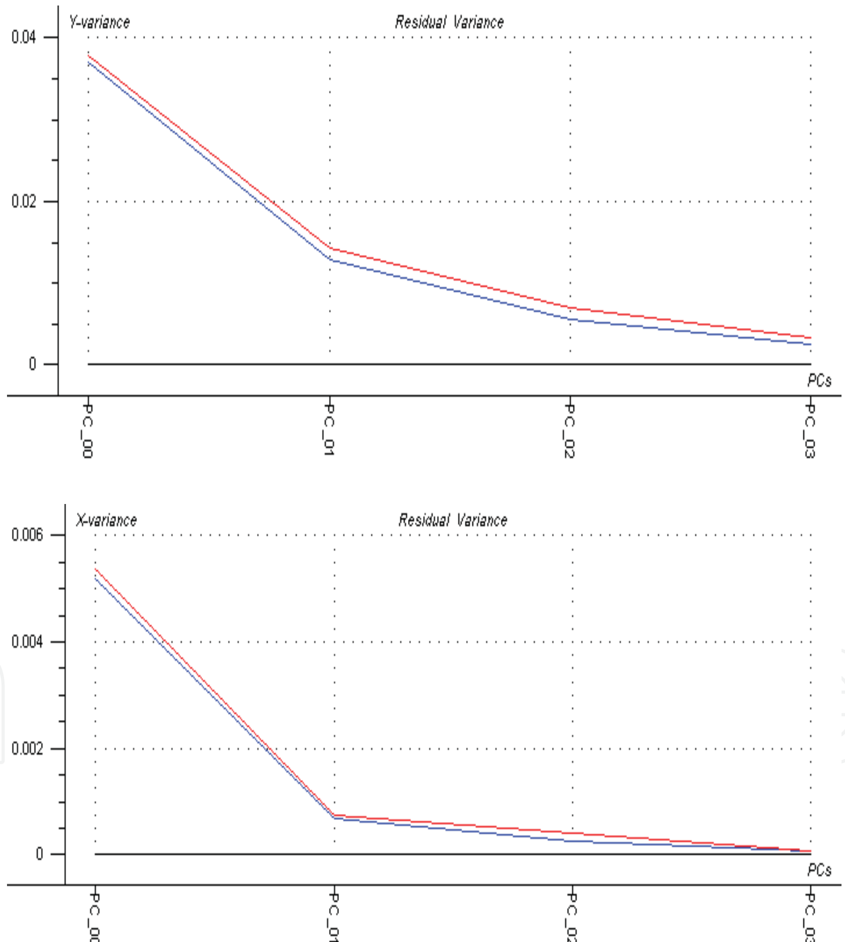


Fig. 13. Result of PLSR modeling for volumetric shrinkage showing: Residual variances (blue during calibration and red during prediction) exhibiting the remaining variation that is not taken into account by the model is minimum after fitting three PLS components suggesting much of the variability in volumetric shrinkage is explained by the model. The upper graph shows Y-variance and the lower graph shows the X-variances.

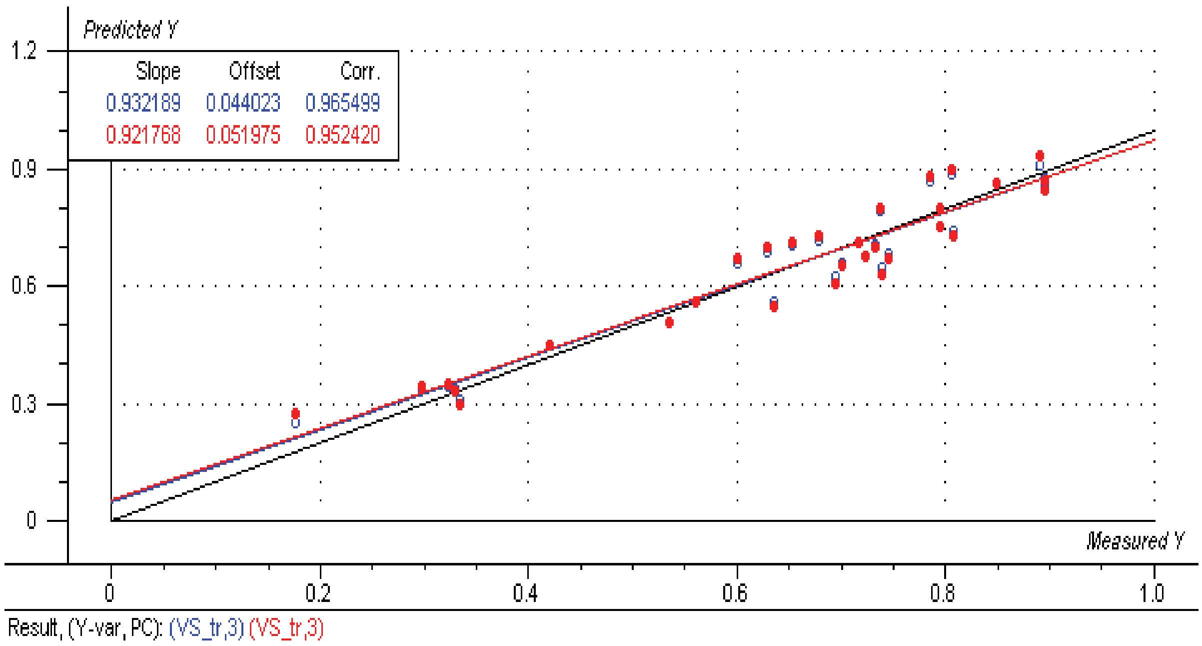


Fig. 14. Result of PLSR modeling for volumetric shrinkage showing: Regression overview showing predicted and measured volumetric shrinkage.

Note that there are no outlying samples lying outside the rest of the cloud (Figure 11). Only one sample lies outside the ellipse; under normal situation it is expected that about 5 % of the samples to lie outside the ellipse.

As shown in Figure 12 Relevant X variables (wavelengths from soil spectra) in predicting volumetric shrinkage fall in the VNIR and SWIR regions. Wavelengths in the SWIR bands are related with clay mineral diagnostic features (Clark, 1999). Wavelengths from the VNIR can be organic matter and iron oxides related (Ben-Dor and Banin, 1994; Wan et al., 2002) and sand or quartz related spectral features (Viscarra et al., 2006).

Figure 13 shows that most of the Y and X variances are accounted for by the three PLS factors, reaching a minimum level (close to zero) of unexplained variances at the third PLS factor. The blue and the red lines represent residual variances during the calibration and validation stages respectively. Note that the two lines do not significantly differ indicating that the calibration data are well fitted and that the model describes the validation data equally well.

In the regression overview (Figure 14) comparing laboratory measured and corresponding predicted (from spectral reflectance of soil samples using PLSR analysis) soil volumetric shrinkage magnitudes, calibration and prediction points lie very close to each other suggesting the model fitted to the calibration data set described the prediction data set as good as possible. Note that an internal calibration, full cross validation leave one out at a time method was used.

Apart from high coefficient of determination (~0.91), the model gives low estimation errors during the calibration (RMSEC = 0.05) as well as the validation (RMSEP = 0.06) stages. Standard errors of calibration (SEC = 0.05) and prediction (SEP = 0.06) which are indicators of precision of the calibration and prediction respectively are also small. The bias which is the average value of the difference between the predicted and measured values, is also small (both in the calibration and prediction stages) for the given number of PLS factors indicating that the effect of bias is negligible (Martens and Naes, 1989). The values of offsets in the calibration and validation stages are small showing minor deviation from an ideal line where the measured and predicted volumetric shrinkage magnitudes are expected to be equal. Model performance indices are presented in Table 4.

| Calibration | | | | | Validation | | | | |
|---|---|---|---|---|---|---|---|---|---|
| Correlation coefficient | RMSEC | SEC | Bias | Offset | Correlation coefficient | RMSEP | SEP | Bias | Offset |
| 0.965 | 0.05 | 0.05 | 0.005 | 0.044 | 0.952 | 0.586 | 0.0596 | 0.001 | 0.051 |

Table 4. Summary of model performance indices resulted from PLSR modeling of soil volumetric shrinkage.

## 4. Conclusions

In this chapter we demonstrated that it is possible to estimate soil volumetric shrinkage from spectral reflectance of soil. The approach can be of potential geotechnical utility contributing to the quality of geotechnical investigations of expansive soil, playing prominent role in planning and designing of infrastructure. This is particularly in minimizing uncertainties through identifying geotechnically problematic areas and estimation of critical parameters (in this case volumetric shrinkage), hence providing better basis for decision making. This in turn present relevant information that can be useful in site selection, route planning and search for construction materials (borrow, subbase etc) especially in the reconnaissance and preliminary design stages of construction projects. In summary;

- The expansive soils in this study are identified by their constituent dominant clay mineral type and accordingly classified into two clusters. Those soils comprised of active clay mineral smectite exhibit high swell-shrink potential as suggested by the magnitude of volumetric shrinkage, plasticity and other related geotechnical characteristics. They also exhibit low maximum dry densities while their optimal moisture contents are high. Halloysite clay mineral dominated soils on the other hand show less swell-shrink susceptibility, and variable maximum dry densities with optimum moisture contents lower than those exhibited by the smectite dominated soil samples. Some halloysite bearing soils can be weak and show high swell-shrink susceptibility as indicated by their geotechnical properties. Note their CBR strengths presented in Figure 7 for the wettest likely condition likely and the associated CBR swell that they exhibited coupled with values of volumetric shrinkage and plasticity characters that they show. Quartz dominated soil samples on the other hand show higher maximum dry density with low moisture intake. These soils also attain high CBR strength and show negligible CBR swell.
- Differences in geotechnical characteristics show dependency on clay mineralogy among different species (smectite, halloysite), and on clay fraction among similar varieties in the studied soils. The fact that clay mineralogy is a crucial factor dictating a number of soil geotechnical behaviors laid emphasis on the importance of qualitative clay mineralogical assemblage analysis of expansive soils. Since spectroscopy is a cheap, rapid and non-destructive way of analyzing soil mineralogy, it can be used for such kind of routine analysis in order to complement quantitative analyses.

- Coefficient of determination obtained in the PLSR analysis show that soil volumetric shrinkage is highly correlated with spectral parameters. The low estimation and interference errors, negligible bias and small offsets indicate spectroscopic techniques potential to be used in routine quantitative analyses of soil shrinkage potential. The presented empirical relations with the added valuable information on the content of major clay minerals (from spectral interpretations) establish a simple way of characterizing expansive soils. Despite the complex nature (comprised of various constituents other than clay materials which are responsible for their expansive characteristics) of soil the results proved that a remarkable amount of information about soil properties can be obtained from their reflectance spectra.
- The current study gave an outlook for future application of optical remote sensing to map soils susceptible to swell-shrink and variation in the magnitude of expansion and shrinkage, provided with the availability of sufficiently high resolution (both spatially and spectrally in order to resolve vital spectral details ) data.

## 5. References


Abebe, Franscesco, Fabrizio and Piero, 1999. Geological Map of Debreziet Area (Ethiopia). GSE, Addis Ababa.

Al-Rawas, A.A., 1999. The factors controlling the expansive nature of the soils and rocks of northern Oman. Engineering Geology, 53: 327-350.

ASD, 1995. Analytical Spectral Devices (ASD): Technical Guide, Portable Spectroradiometers, Analytical Spectral Devices, Inc.

AusSpec International, 2005. The Spectral Geologist software. AusSpec Interbational, Sydney.

Ben-Dor, E. and Banin, A., 1994. Visible and Near-Infrared (0.4-1.1μm) analysis of Arid and Semiarid Soils Remote Sensing of Environment, 48: 261 - 274.

CAMO, 2005. The unscarmbler 9.2.

Chabrillat, S., Goetz, A.F.H., Krosley, L. and Olson, H.W., 2002. Use of hyperspectral images in the identification and mapping of expansive clay soils and the role of spatial resolution. Remote Sensing of Environment, 82: 431 - 445.

Clark, R.N., 1999. Spectroscopy of Rocks and Minerals, and Principles of Spectroscopy. In: A. Rencz (Editor), Chapter 1 in: Manual of Remote Sensing. John Wiley and Sons, Inc, New York.

Crowley, J.K. et al., 2003. Spectral reflectance properties (0.4-2.5 μm) of secondary Fe-oxides, Fe-hydroxides, and Fe-sulphate-hydrate minerals associated with sulphide -bearing mine wastes. Geochemistry; Exploration, Environment, Analysis, 3: 219-228.

Erguler, Z.A. and Ulusay, R., 2003. A simple test and predictive models for assessing swell potential of Ankara (Turkey) clay. Engineering Geology, 67: 331 - 352.

FAO, 1998. World reference base for soil resources. International Society of Soil Science, Rome.

Fitzpatrick, E.A., 1980. SOILS; their formation, classification and distribution. Longman Inc., London, NY, 354 pp.

Goetz, A.F.H., Chabrillat, S. and Lu, Z., 2001. Field Reflectance Spectrometery for Detection of Swelling Clays at Construction Sites. Field Analytical Chemistry and Technology, 5(3): 143-155.

Gourley, C., Newill, D. and Schreiner, H.D., 1993. Expansive soils: TRL's research strategy, First International Symposium on Engineering Characteristics of Arid Soils. Overseas Centre, Transport Research Laboratory, Crowthorne, Berkshire, UK., City University, London.

Hocking, R.R., 2003. Methods and Applications of Linear Models Regression and the analysis of variance. Wiley series in probability and statistics.

Kariuki, P.C., Woldai, T. and Van der Meer, F.D., 2004. Effectiveness of spectroscopy in identification of swelling indicator clay minerals. International Journal of Remote Sensing, 25(2): 455 - 469.

Kooistra, L., 2004. Incorporating spatial variability in ecological risk assessment of contaminated river floodplains. PhD Thesis, Katholieke Universiteit Nijmegen, Nijmegen, The Netherlands.

Martens, H. and Naes, T., 1989. Multivariate Calibration. John Wiley & Sons, INC.

Nelson, J.D. and Miller, D.J., 1992. Expansive Soils Problems and Practice in Foundation and Pavement Engineering. John Wiley & Sons, Inc.

Ramana, K.V., 1993. Humid tropical expansive soils of Trinidad: Their geotechnical properties and areal distribution. Engineering Geology, 34: 27 - 44.

Shi, B., Jiang, H., Liu, Z. and Fang, H.Y., 2002. Engineering geological characteristics of expansive soils in China. Engineering Geology, 67: 63 - 71.

Snethen, D.R., 1975. A Review of Engineering Experiences with Expansive Soils in Highway Subgrades, Fedral Highway Administration Office of Research and Debvelopment, Washington D.C.

Takahashi, T., Dahlgren, R.A., Theng, B.K.G., Whitton, J.S. and Soma, M., 2001. Potassium-Selective, Halloysite-Rich Soils Formed in Volcanic Materials from Northern California. Soil Science Socaitey of America, 65: 516 - 526.

Van der Meer, F.D., 1999. Can we map swelling clay with remote sensing? International Journal of Applied Earth Observation & Geoinformation (JAG), 1: 27-35.

Viscarra, R.A.R., Walvoort, D.J.J., McBratney, A.B., Janik, L.J. and Skjemstad, J.O., 2006. Visible, near infrared, mid infrared or combined diffuse reflectance spectroscopy for simultaneous assessment of various soil properties. Geoderma, 131: 59 - 75.

Wan, Y., Kwong, J., Brandes, H.G. and Jones, R.C., 2002. Influence of Amorphous Clay - Size Materials on Soil Plasticity and Shrink - Swell Behaviour. Journal of Geotechnical and Geoenvironmental Engineering, 128: 1026 - 1031.

West, S.L., Juo, A.S.R., White, G.N., McInnes, K.j. and Dixon, J.B., 2004. Kaolinite, Halloysite, and Iron Oxide Influence on Physical Behavior of Formulated Soils. Soil Science Socaitey of America, 68: 1452 - 1460.

Wold, S., Sjostrom, M. and Eriksson, L., 2001. PLS-regression: a basic tool of chemometrics. Chemometrics and Intelligent Laboratory Systems, 58: 109-130.

Yitagesu, F.A., Van der Meer, F.D. and Van der Werff, H., 2009. Quantifying engineering parameters of expansive soils from their reflectance spectra. Engineering Geology, 105: 151 - 160.

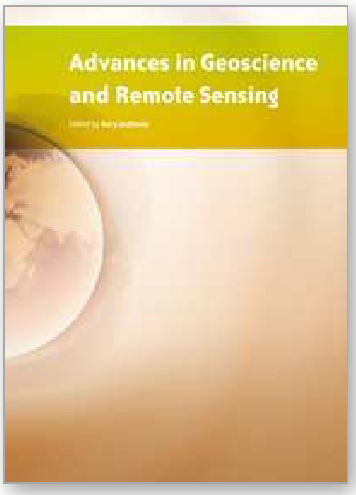


**Advances in Geoscience and Remote Sensing**

Edited by Gary Jedlovec

ISBN 978-953-307-005-6

Hard cover, 742 pages

**Publisher** InTech

**Published online** 01, October, 2009

**Published in print edition** October, 2009

Remote sensing is the acquisition of information of an object or phenomenon, by the use of either recording or real-time sensing device(s), that is not in physical or intimate contact with the object (such as by way of aircraft, spacecraft, satellite, buoy, or ship). In practice, remote sensing is the stand-off collection through the use of a variety of devices for gathering information on a given object or area. Human existence is dependent on our ability to understand, utilize, manage and maintain the environment we live in - Geoscience is the science that seeks to achieve these goals. This book is a collection of contributions from world-class scientists, engineers and educators engaged in the fields of geoscience and remote sensing.

**How to reference**

In order to correctly reference this scholarly work, feel free to copy and paste the following:

Fekerte Arega Yitagesu, Freek van der Meer and Harald van der Werff (2009). Prediction of Volumetric Shrinkage in Expansive Soils (Role of Remote Sensing), Advances in Geoscience and Remote Sensing, Gary Jedlovec (Ed.), ISBN: 978-953-307-005-6, InTech, Available from: http://www.intechopen.com/books/advances-in-geoscience-and-remote-sensing/prediction-of-volumetric-shrinkage-in-expansive-soils-role-of-remote-sensing-

INTECH
open science | open minds

**InTech Europe**
University Campus STeP Ri
Slavka Krautzeka 83/A
51000 Rijeka, Croatia
Phone: +385 (51) 770 447
Fax: +385 (51) 686 166
www.intechopen.com

**InTech China**
Unit 405, Office Block, Hotel Equatorial Shanghai
No.65, Yan An Road (West), Shanghai, 200040, China
中国上海市延安西路65号上海国际贵都大饭店办公楼405单元
Phone: +86-21-62489820
Fax: +86-21-62489821

© 2009 The Author(s). Licensee IntechOpen. This chapter is distributed under the terms of the Creative Commons Attribution-NonCommercial-ShareAlike-3.0 License, which permits use, distribution and reproduction for non-commercial purposes, provided the original is properly cited and derivative works building on this content are distributed under the same license.